Advances in Science and Technology Research Journal

Advances in Science and Technology Research Journal 2022, 16(3), 78–88
https://doi.org/10.12913/22998624/148167
ISSN 2299-8624, License CC-BY 4.0

Received: 2022.02.17
Accepted: 2022.04.20
Published: 2022.05.15

Effect of Surface Tilt on Nanoindentation Measurement on Copper and Glass

Jarosław Borc[1]

[1] Department of Applied Physics, Lublin University of Technology, ul. Nadbystrzycka 38, 20-618 Lublin, Poland
E-mail: j.borc@pollub.pl

ABSTRACT

Results of an investigation of the effect of surface tilt in range of 0°–6° on nanoindentation measurements under Berkovich indenter at different loads made on copper and glass surfaces are presented and discussed. It was found that: (1) measured hardness increases for tilt angle $\theta > 3°$ and this increase is about 12% at $\theta = 6°$ for both samples at all applied loads, (2) the overestimation in hardness is due to the increase of projected contact area A with the tilt angle θ, but the theoretical contact area A described by the traditional analytical area function leads to lower change in the hardness than the experimental one up to about 5% may be attributed to the horizontal deflection of the stem holding the indenter, and (3) indentation modulus E is more sensitive to the tilt for glass than copper and the sensitivity in the values of E at a given tilt angle θ increases with decreasing indention load.

Keywords: indentation test, hardness, measurement, mechanical properties.

INTRODUCTION

In the last few years indentation of solids at very low loads, referred to as nanoindentation, has drawn increasing interest. This is a modern depth-sensing technique, which allows to measure hardness, elastic modulus and plasticity of materials. The technique is based on the registration of the dependence of indenter depth on applied load during a loading and unloading indentation cycle. Since the process of unloading of the indenter is elastic, the analysis of the unloading curve enables to define elastic modulus of the tested sample. It is well known that the results of indentation testing depend on the conditions under which the measurement is made. For example, the apparent microhardness of solids depends on the applied indentation test load. This phenomenon, known as the indentation size effect (ISE), has been widely investigated and discussed (for example, see refs. [1–3]). Indentation methods are, in general, sensitive to the position of investigated surface relative to the axis of indenter tip. Therefore, it is necessary that part of the specimen surface where indentation is made is flat and oriented horizontally, i.e. it is perpendicular to the axis of the indenter. However, in practice, precise position of surfaces of specimens is difficult to attain especially when a specimen is uneven or rough. From the standpoint of the researcher it is interesting to understand the influence of tilt of investigated surface on the accuracy of measurements.

During the last decade several works have studied the effect of sample tilt on nanoindentation deformation of materials. Using finite element simulation and nanoindentation experiments with conical indenter, Xu and Li [4] showed that indentation on a tilted sample results in: (i) a higher load necessary to penetrate the same depth, (ii) a larger contact area A in the same penetration depth h, and (iii) a larger contact stiffness S. According to these authors, a significant underestimation in contact area A leads to a significant overestimation in hardness H (130%) and elastic modulus E (50%). Analogous simulations was made by Gao et al. [5] but for spherical indenter. Zhong et al. [6] made the experiment using spherical-conical indenter with tilt angle from 5° to 30°.

The authors shows that the spherical geometry and cone profile of the indenter made effects in the indentation and scratching process simultaneously when tested samples were tilted. However, these authors did not provide specific data describing the differences in the results obtained for various tilt angle. In contrast to this Kashani and Madhavan [7, 8] proposed a geometric correction procedure for Berkovich indentation based on the derived projection area function given by

$$A = \frac{2\sqrt{3}h_c^2 \tan^2\varphi}{1-3\tan^2\varphi\tan^2\theta-2\tan^3\varphi\tan^2\theta\cos 3\zeta} \quad (1)$$

where: ϕ is the face angle of the indenter, θ is the sample tilt angle and ζ is the rotation angle (see Figure 1).

The authors verified the accuracy of the geometric correction of the area function for indentation into tilted samples by the results of three-dimensional (3D) simulations for both pile-up and sink-in materials. These authors also reported that, if the standard area function (Equation (3)) is used, the contact area is underestimated, leading to 8% overestimation in hardness and 4% overestimation in elastic modulus. These overestimated values are much lower than those reported in ref. [4]. Moreover, overestimation in hardness is about 5% lower than that predicted from Equation (1). The authors hypothesised that it is due to slight deflection of the stem holding the indenter in the horizontal direction. This deflection causes the actual penetration depth to be lower than that measured by the instrument and counteracts the error due to the underestimation of indentation contact area of tilted sample. Shi et al. [9] used finite element analysis of Berkovich indentation to show that at the maximum indentation depth a 5°-tilted face results in a 25% increase projected contact area whereas the hardness and elastic modulus are, respectively, about 17.8 and 13.4% higher than those obtained for the untilted face. Similar studies were carried out by Wang and Liu [10] where nickel-boron with a sinusoidal surface was used as samples. The result shows that the errors caused by 2.5 degrees tilt are 4% in elastic modulus and 11% in hardness. A quantitative model, fitted on experimental results on stainless steel made by Laurent-Brocq et al. [11], established criteria that hardness measurements with an uncertainty lower than 10% is guaranteed if the surface tilt is lower than 2°. Jakes and Staufer [12] made investigation on PMMA samples using Berkovich indenter with applied load of 1–12 mN. The authors used a geometric model to create contour plots from which the area correction factor can be directly determined using only the ratios of side lengths measured from an image of the triangular nanoindentation impression. The effectiveness of the correction method was demonstrated by successfully correcting hardness and elastic modulus measurements with surface tilts as high as 6°. However, according to the authors, the geometric correction factor may not work as well if the pile-up behaviour is affected by surface tilt and different sides of the triangular nanoindentation impression have different amounts of pile-up. It should be noted that the edges of the imprints used in the measurements were almost perfectly straight.

The above survey on the effects of sample tilt on nanoindentation of different types of samples shows that there is relatively high discrepancy between the experimental results and theoretical predictions and that differences occur between the results obtained for more plastic (pile-up) and more elastic (sink-in) samples. The aim of this work is to study the effect of sample surface tilt on nanoindentation hardness and modulus for glass and copper samples as representative of elastic and plastic materials and to explain the large discrepancy between the theoretical and experimental data. An additional aim is to investigate the phenomenon at loads up to 30 mN not used for Berkovich indenter in the previous studies.

MATERIAL AND METHODS

Nanoindentation tests were carried out using the Ultra Nano Hardness Tester (UNHT) with a diamond Berkovich indenter developed by CSM Instruments (Switzerland) fitted to a digital camera. The main improvements are a new tip and reference fixing system introduced in Ultra Indenter Head and using active top referencing possibility (very low loads less than 10 mN applied by the reference) for depth and load measurements, no temperature effect, feedback loop control of the load applied by the reference and by the indenter, low thermal drift, high resonance frequency, one order less noise level, and new electronic design. All these advantages that this UNHT with high performance allows in making measurements are not possible to be attained by conventional nanohardness tester.

The indentation experiment was performed on two samples: (1) commercial 99.99% copper plate and (2) commercial microscope glass slide. The tested samples were flat and smooth but the copper specimen was polished mechanically before indentation testing. The specimens were fixed in the tip-tilt stage produced by Edmund Optics Ltd, with travel angle ±3° and 74 arcsec resolution. Indentation tests were carried out at room temperature changing the tilt angle θ from 0° to 6° with interval of 0.5°. Schematic illustration of the experimental setup is presented in Figure 1. While using the reference the sample surface must be parallel to the x axis and the sample rotation was made with respect to this axis. In this respect all measurements were made taking the rotation angle $\zeta = 30°$ between the y axis and the impression contact length from its deepest point (see Figure 1). Experiments were carried out at maximum test loads F_m of 10, 30 and 50 mN and an indentation dwell time of 20 s with loading/unloading rate of 30 mN/min. For each value of tilt angle θ, five indentations were performed at a particular load. To avoid surface effects during the measurements the separation between neighbouring indentations was kept more than six times the diagonal length of indentation impressions.

Additionally, the roughness of the tested surfaces was determined in order to determine its influence on the accuracy of the measurements. To determine the surface roughness the CSM Nano Scratch Tester tester was used as a profilometer with the scanning load of 0.2 mN.

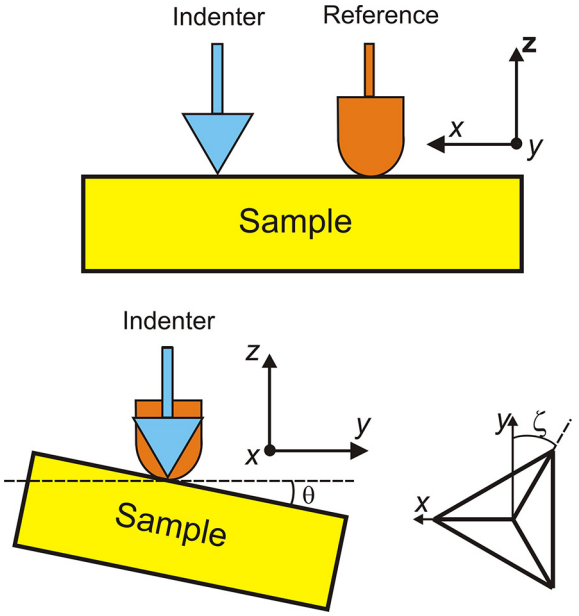

Fig. 1. Schematic illustration of nanoindentation experiment. In the figure θ is the sample tilt angle, and the rotation angle $\zeta = 30°$ is along the z axis (see text)

RESULTS AND DISCUSSION

Theoretical background

The values of the hardness H, the elastic modulus E and the reduced modulus E_r of the samples were computed using the software supplied with the UNHT. This software calculates hardness H, in this case called indentation hardness H_{IT}, using the standard relation

$$H_{IT} = F/A \tag{2}$$

where: F is the applied load and A is the projected indentation impression area determined from contact depth h_c, which is the distance between indentation depth under test force and surface profile under load.

In the case of Berkovich indenter the projected area is given by

$$A_p = 2\sqrt{3}h_c^2 \tan^2 \varphi \tag{3}$$

where: $\phi = 65.27°$ is the face angles of regular pyramid.

Because the tip of an indenter is not ideally sharp, the projected area is described by the relation

$$A_c = C_0 h_c^2 + C_1 h_c + C_2 h_c^{1/2} + \ldots + C_5 h_c^{1/16} \tag{4}$$

where: the constants C_0, C_1, …, C_5 are determined by instrument calibration according to Oliver and Pharr [13].

The contact depth h_c and elastic (indentation) modulus E are calculated using the Oliver-Phaar (O-P) method [13] from expressions as follows:

$$h_c = h_m - \varepsilon \frac{F_m}{S} \tag{5}$$

$$\frac{1-\nu^2}{E} = \frac{1}{E_r} - \frac{1-\nu_i^2}{E_i} \tag{6}$$

where: h_m and F_m are the maximum penetration and the maximum load, respectively, ε depends mainly on the indenter shape and depend only to a small extent on the material properties, S is the stiffness calculated from the tangent fit dF/dh of unloading curve and the reduced modulus.

$$E_r = \frac{S\sqrt{\pi}}{2k\sqrt{A_c}} \tag{7}$$

In the above equations v and n_i are the Poisson ratio of the sample and indenter, respectively, E_i is the elastic modulus of the indenter and the geometrical factor $k = 1.034$ for the Berkovich indenter.

The projected contact area A as a function of tilt angle η and rotation angle ζ (see Figure 1) was calculated by using relation (1) and hardness H_{IT} and elastic modulus E of glass and copper samples were determined. However, the hardness H_{IT} and elastic modulus E determined in this way still showed large deviations for relatively high tilt angle.

Roughness measurements

The mean roughness value R_a of each sample was calculated with over five on different regions of the substrate surface. Examples of the 0.5 mm length profiles of the copper and glass surfaces are shown in Figure 2. The results of R_a values and the percentage ratio R_a/h_m, where h_m is the maximum penetration depth of indentation obtained for given maximum indentation test load F_m are given in Table 1. On the basis of the results of the Table it can be concluded that the effect of roughness on the indentation results can be neglected because the value of roughness R_a is in each case less than 5% of the value of maximum of penetration h_m).

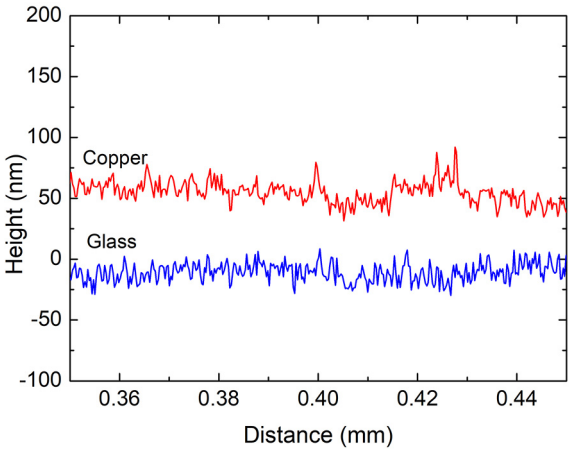

Fig. 2. Examples of surface profiles made on the copper and glass samples

General features of load-displacement curves

Examples of Berkovich nanoindentation imprints produced on glass and copper faces at a maximum test load of 50 mN made for known values of the tilt angle θ are presented in Figure 3. The x, y and z axes indicated in the photographs are oriented following the convention used in Figure 1. It can be seen that the boundaries of the imprints are not equilateral triangles but are concave inwards and convex outwards for the glass and copper samples, respectively. The former type of imprints occur for sink-in and the latter for pile-up materials. Moreover, it was observed from indentation experiments that asymmetry in the imprints shape becomes more with increasing values of angle θ. This phenomenon always occurs when the specimen surface is not exactly perpendicular to the vertical axis of the indenter. An elongation in the imprint shape (see Figure 3) occurs along the y axis on the sides of the specimen lying above the indentation contact point and a contraction occurs below this point.

Figure 4 shows examples of load-displacement F-h curves obtained on copper and glass surfaces for tilt angles $\theta = 0°$, 3° and 6° for the maximum test load of 30 mN. As seen from the figure, the values of penetration on both samples are low for higher tilt angle. This leads to overestimation of the hardness for tilted samples

Indentation hardness

The experimental results of hardness H_{IT} as a function of surface tilt angle θ obtained for various maximum test loads performed on copper and glass surfaces reveal apparent increase in hardness

Table 1. Mean surface roughness values R_a and their percentage in maximum indentation depth h_m of the copper and glass samples

Copper				Glass			
R_a	R_a/h_m	F_m	h_m	R_a	R_a/h_m	F_m	h_m
nm	%	mN	nm	nm	%	mN	nm
16	1.2	50	1320	4.5	0.6	50	760
-	1.6	30	1030	-	0.8	30	570
-	2.9	10	550	-	1.4	10	320

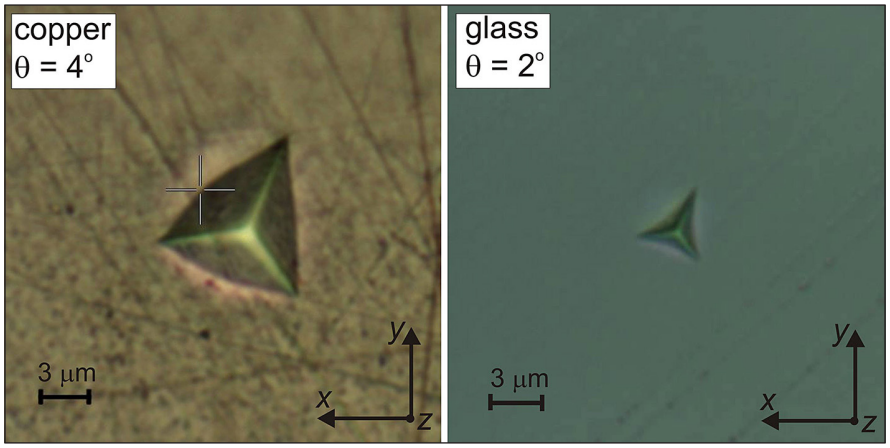

Fig 3. Examples of Berkovich indentation imprints produced on copper and glass samples at 50 mN maximum test loads made for known tilt angle θ

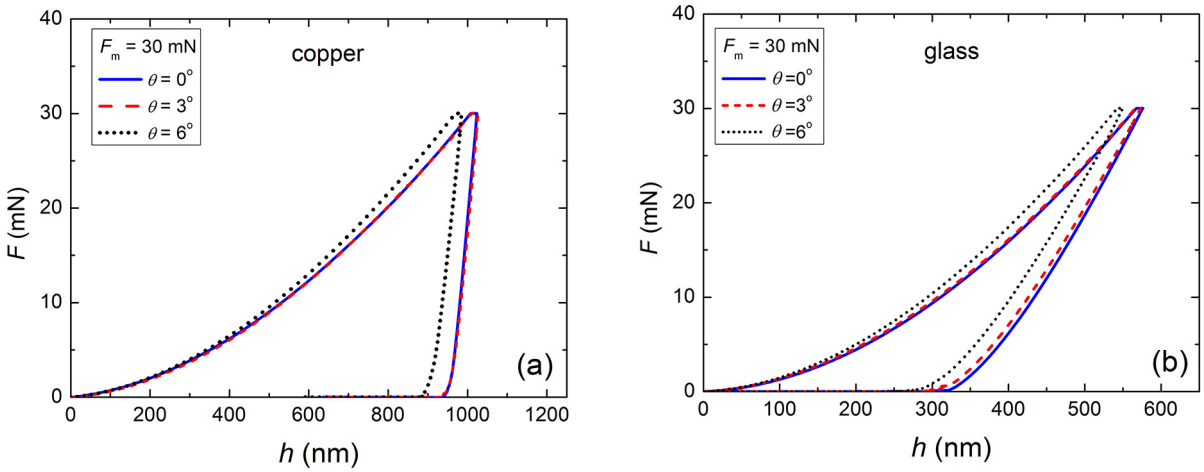

Fig. 4. Examples of load-displacement (*F*-*h*) curves obtained for three different sample tilt angles θ on (a) copper and (b) glass samples

with increasing tilt angle. Dependence of normalized hardness presented as a ratio of hardness of tilted sample H_{IT} and without tilt H_{IT0}, on the tilt angle θ obtained for maximum test loads of 10, 30 and 50 mN made on the copper and glass surfaces are indicated as "exper." in Figure 5. As seen from the Figure 5. for a given test load, the mean values of apparent hardness H_{IT} are practically constant for $0° < \theta < 3°$. For $\theta = 0°$, these values are 1.84±0.07, 1.56±0.06 and 1.42±0.10 GPa at 10, 30, 50 mN, respectively, in the case of copper, whereas they are 8.12±0.09, 8.34±0.31, and 8.15±0.09 GPa at 10, 30 and 50 mN, respectively, in the case of glass. It should be noted that the value of H_{IT} of the copper specimen decreases with an increase in the maximum applied load F, in all range of angle θ. This phenomenon is representative of normal indentation size effect (ISE), and is in agreement with the reported normal ISE of copper [15]. However, in the case of glass the ISE phenomenon is difficult to distinguish. The ISE phenomenon is widely studied (for example, see refs. [1–3]) and is not the subject of this study.For $\theta > 3°$, the apparent hardness H_{IT} of both samples gradually increases with increasing θ. The scatter in the experimental data is higher in the case of copper. It may be attributed to granular structure of metal and higher roughness of its surface. The influence of roughness on nanoindentation measurements is described in ref. [11]. It may be seen from the figures that the increasing trends of the plots of H_{IT}/H_{IT0} against θ are similar for all applied loads. In the case of copper, for $0° < \theta < 3$ the value of H_{IT}/H_{IT0} fluctuates around 1 with deviations of +4% and –6% but for $\theta > 3°$ its value gradually increases up to about 12% at $\theta = 6°$. Similarly, in the case of glass, for $0° < \theta < 3°$ the deviation in H_{IT}/H_{IT0} is smaller and is ±2.5%, but

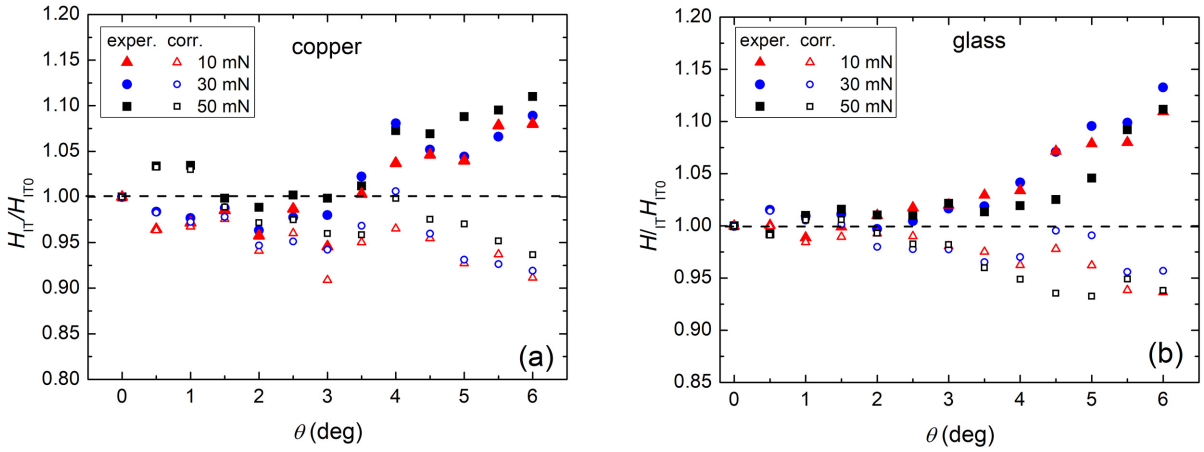

Fig. 5. Dependences of normalized hardness H_{IT}/H_{IT0} and their corrected values on tilt angle θ obtained for maximum test loads of 10, 30 and 50 mN made on (a) copper and (b) glass samples

for $\theta > 3°$ its value increases up to 13% at $\theta = 6°$. The results presented in Figure 5 show that the tilt of the tested surface causes a distinct increase in the measured hardness for surface tilt θ exceeding about 3° and the relative increase in the measured hardness is comparable for the applied loads of both samples. The above results are in good agreement with the simulation results obtained for fused quartz [4, 8, 9]. The overestimation of experimental hardness was also revealed for fused quartz [8] and steel [11]. Kashani and Madhavan [8] found that simulation made for $\theta = 5°$ overestimes hardness by about 10%. As shown in Figure 3, the impression of triangular pyramidal indenter for the tilted sample corresponding to the average contact depth h_c is not an equilateral triangle. The projected contact area in this case is a function of tilt angle θ and rotation angle ζ (see Figure 1) and is described by Equation (1). These authors applied correction procedure by dividing the usual area function A_p of Equation (3) for the normal indentation by the denominator of Equation (1). The results of normalized experimental hardness H_{IT}/H_{IT0} of our copper and glass samples made for three applied loads corrected by following this procedure are included in Figure 5a and b and are indicated as "corr.". It may be seen that the value of the corrected H_{IT}/H_{IT0} decreases with an increase in the angle θ . At θ = 6°, this decrease is about 6%, 8% and 9% for loads of 10, 30 and 50 mN, respectively, in the case of copper. These values lie between 4% and 6% in the case of glass. From these results it may be concluded that the experimental overestimation in the hardness of the tilted samples is lower than the theoretical predictions from Equation (1). Following Kashani and Madhavan [8], the theoretical dependence of normalized projected area, presented as the A/A_p ratio of contact area A with tilt (Equation (1)) and without tilt A_p (Equation (3)), on the rotation angle

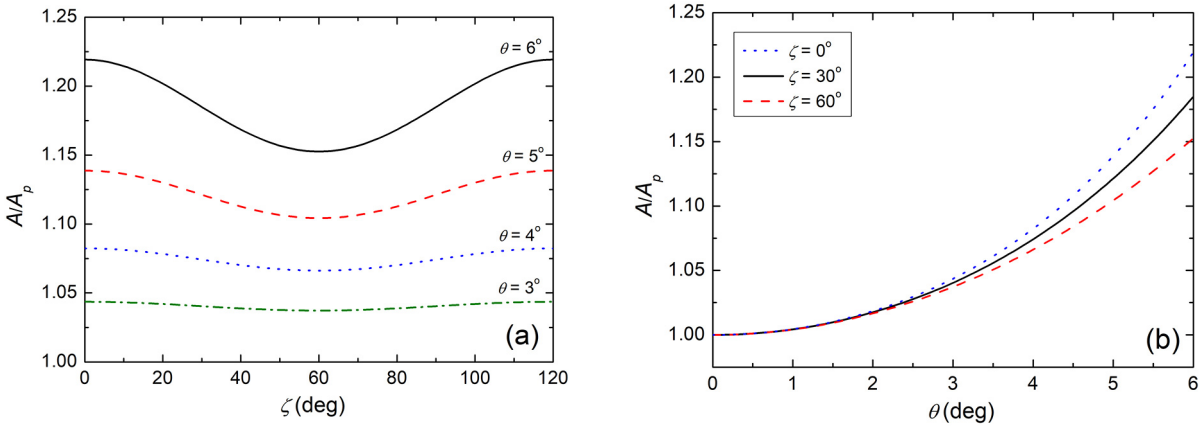

Fig. 6. Dependence of theoretical normalized projected contact area of Berkovch indenter on: (a) rotation angle ζ and (b) tilt angle θ plotted according to Equation (1)

ζ for various tilt angle θ is presented in Figure 6a. This dependence shows that the error of the projected area due to tilt varies from a minimum at ζ = 60° to a maximum at ζ = 0°. In the latter case, the sample tilt is along the edge of the pyramid. It may be seen that this deviation increases with an increase in the tilt angle θ. This behavior is clearly seen in Figure 6b, where the dependence of the normalized projected area A/A_p on the angle θ is presented for various angles ζ. The difference in the deviation of the projected area calculated for ζ = 0° and 60° increases with an increase in the tilt angle θ. However, this difference for θ ranging from 0° to about 3° is negligible. The dependencies presented in Figure 6 show that the normalized projected area A/A_p for ζ = 30°, applied in this study, increases by 17% for θ = 6°. Since the projected area calculated by the instrument is lower than that of the real imprint produced on the tilted surface, the experimental hardness apparently increases when the tilt angle θ increases. It should be noted that the increase in A/A_p presented in Figure 6 is about 5% higher than the experimental normalized hardness presented in Figure 5.

The results presented above suggest that there are other factors responsible for the underestimation of the projected area A. Since the hardness obtained by the O-P method uses the penetration depth described by Equation (5), it was verified whether stiffness S affects underestimation in the projection area. For this purpose, the projected contact area $A(h_m)$ corresponding to the maximum penetration h_m obtained from the experiment was calculated, omitting the second factor of Equation

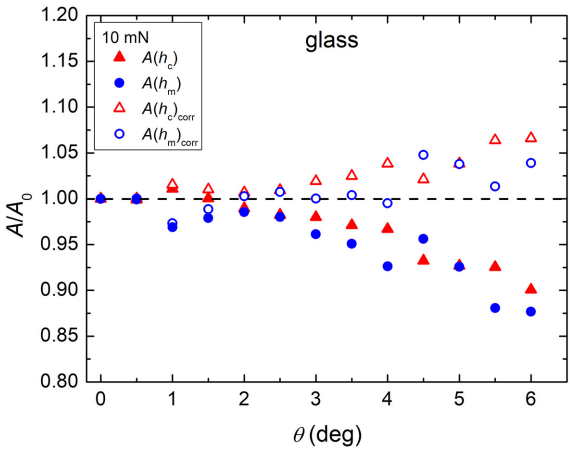

Fig. 7. Dependence of experimental normalized projected contact area with and without tilt corrections on tilt angle θ obtained for maximum test load of 10 mN made on the glass sample

(5), as a function of the maximum penetration h_m. Figure 7 presents, as an example, the dependence of the normalized projected area $A(h_m)/A_0(h_m)$, with the $A(h_c)/A_0(h_c)$, where $A(h_c)$ is the projected contact area obtained from the device using Equation (4), on the tilt angle θ obtained at the maximum test load 10 mN on the glass sample. The $A_0(h_m)$ and $A_0(h_c)$ are the data obtained for the untilted sample. Obviously, the decrease in $A(h_c)/A_0(h_c)$ with an increase in the tilt angle θ is due to constant load applied in the experiment. In view of the above, the $A(h_c)$ and $A(h_m)$ data were divided by the denominator of Equation (1). The $A(h_c)$ and $A(h_m)$ data corrected in this way are presented in Figure 7 as $A(h_c)_{corr}/A_0(h_c)_{corr}$ and $A(h_m)_{corr}/A_0(h_m)_{corr}$, using open triangles and open circles, respectively. As seen from the figure, there is no significant differences between these $A(h_c)$ and $A(h_m)$ data. This suggests that the stiffness S of the sample does not lead to the overestimation of the hardness of tiled samples. More detailed analysis of stiffness S of samples is presented in the next section.

The results presented in Figures 5 and 7 show that introduction of the above correction from increase projected contact area with tilt angle at constant penetration depth leads to excessive deviations in the normalized projected contact area. A similar conclusion was reached by Kashani and Madhavan [8]. In order to explain the disagreement these authors speculated that the stem holding the indenter is slightly deflected to the side owing to the side force developed while indenting a tilted specimen. The deflection of the stem moves the indenter in the direction of the slope of the sample surface, causing the actual penetration depth to be smaller than the recorded penetration depth, which would cause the actual area of contact to be smaller than that the estimated based on the recorded penetration depth. Consequently, it is necessary to introduce an additional correction factor to account for the stem deflection. Figure 8 shows the schematic view of indenter deflection d during indentation where h_3 is the penetration depth recorded by the instrument and h_2 is the actual one. It is assumed that path of indentation is along the dropped line inclined at an angle β in relation to the vertical. When the horizontal deflection d is very low relative to the penetration depth, the height $h_3 \approx h_1$. Since the angles β and θ are given by $\tan\beta = d/h_1$ and $\tan\theta = (h_1 - h_2)/d$, the actual penetration depth h_2 may be given by

$$h_2 = h_1(1 - \tan\beta \cdot \tan\theta) \qquad (8)$$

The angle of indentation path β is a function of tilt angle η and is related to individual construction of stem holding the indenter. Therefore, the actual penetration depth h_2 may be written as

$$A = h_1(1 - \tan C\theta \cdot \tan\theta) \quad (9)$$

where: C is a constant characteristic of the indenter-stem holding arrangement. Replacing depth h_2 by h_c in Equation (1), the additional correction is obtained.

It was found that a new normalized hardness H_{IT1}/H_{IT0}, defined as the ratio of the hardness of tilted sample H_{IT1} with a value of $C = 2.5$ and the hardness H_0 without the tilt is independent of the tilt angle θ. The data of the normalized hardness H_{IT1}/H_{IT0} obtained in this way are presented in Figure 9 for the glass and copper samples.

Using the constant $C = 2.5$ in Equation (9) to account for the correction due to the stem deflection one may estimate the maximum deflection $d = h_m \tan(2.5\eta)$. Taking the maximum optical magnification and the maximum penetration $h_m \approx 1200$ nm at load $F = 50$ mN for copper and the maximum tilt $\theta = 6°$, one finds the maximum observable deflection $d \approx 320$ nm. Since the accuracy in the determination of the central position of an imprint in the horizontal plane recorded optically under the same conditions is about 0.5 μm, it is practically impossible to measure the deflection d in this way.

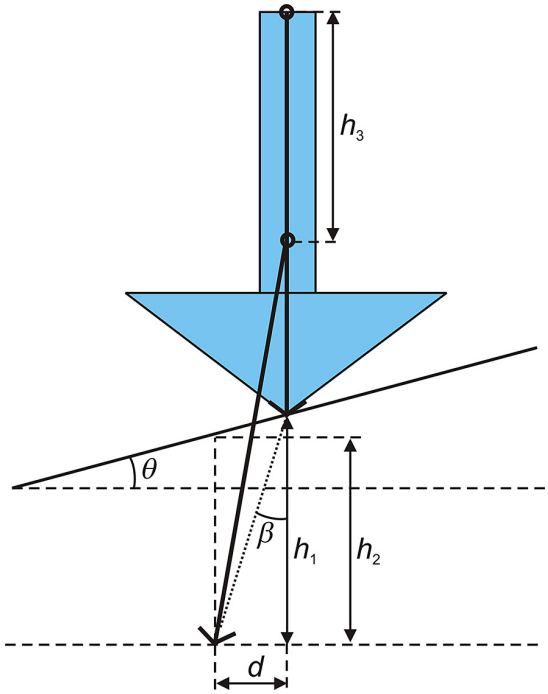

Fig. 8. Schematic illustration of the effect of indenter horizontal deflection d on measured penetration depth h_2 during indentation on tilted sample

Indentation modulus

The experimental results of the indentation modulus E made on the horizontal surface of copper sample reveal that its values decrease with an increase in the applied load and are 116.3±16.5, 87.1±3.6 and 74.2±2.9 GPa for 10, 30, and 50 mN, respectively. The values of the indentation modulus E obtained analogously on the glass sample also show a similar trend and are 78.2±1.0, 72.8±1.3 and 65.6±0.6 GPa for 10, 30, and 50 mN, respectively. For simplicity, the dependencies of normalized reduced modulus E_r (Equation (7)) relative to its value E_{r0} obtained for the horizontal surface as a function of the tilt angle θ were analysed for the copper and

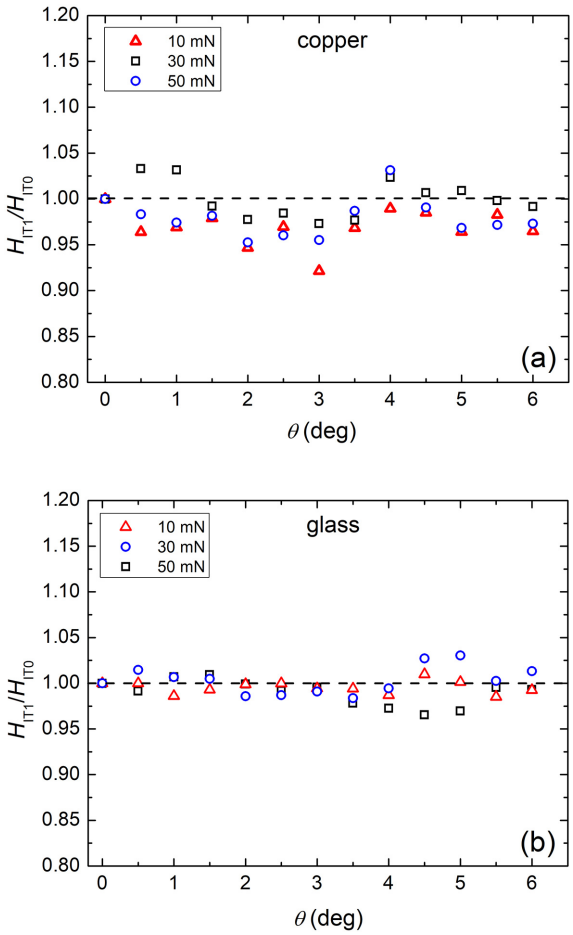

Fig. 9. Dependence of experimental corrected normalized hardness H_{IT1}/H_{IT0} on tilt angle θ obtained for maximum test loads of 10, 30 and 50 mN made on (a) copper and (b) glass samples. Correction was carried out by using Equation (1) where h_c is replaced with h_2 expressed by Equation (9)

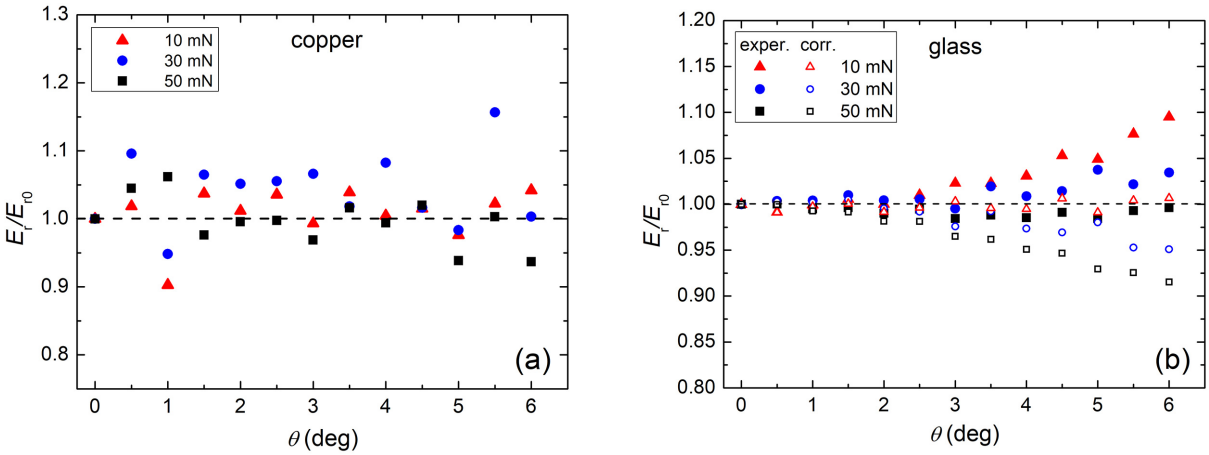

Fig. 10. Dependences of normalized reduced modulus E_r/E_{r0} and their corrected values on surface tilt angle θ obtained for 10, 30 and 50 mN of maximum test loads made on (a) copper and (b) glass samples

glass samples and are presented Figures 10a and b, respectively. It may be seen that the dependence $E_r/E_{r0} = f(\theta)$ reveals no significant trend for the copper sample, but the E_r/E_{r0} values are somewhat lower for large tilt angles at 50 mN (see Figure 10a). A slightly different situation occurs in the case of the glass sample (see Figure 10b), where E_r practically does not change at 50 mN but the values of E_r at 30 and 10 mN increase with the angle θ by 4% and 10%, respectively, for the maximum θ.

The reduced modulus described by Equation (7) is a function of the stiffness S and the projected area A_c for a sample. From a consideration of the results presented in Figure 10, it may be concluded that no universal factor can be applied to the correction in the indentation modulus. The calculated values of E_r for the glass sample using the projected contact area correction, applied above in the case of hardness, are included in Figure 10b. These data are indicated as "corr.". Obviously, these corrected values of E_r depend on the applied load and the best correction is obtained for the 10 mN test load. The effect of the tilt angle θ on the stiffness S is presented as the ratio S/S_0 of stiffness S and S_0 of tilted and untilted samples, respectively, in Figure 11. It may be noted that changes in the stiffness S of the two samples are associated with changes in the reduced modulus presented in Figure 10. However, in the case of glass (Figures 10b and 11b), for $\theta = 6^o$ the values of both E_r and S obtained at 10 mN differ by about 10% from the values obtained at 50 mN. In the figure the values of E_r/E_{r0} are seen to be moved upward relative to those of S/S_0 due to small influence of A/A_0 (cf. Figure 7). Changes in reduced modulus of tilted samples suggest that its sensitivity to the tilt angle is higher for more elastic samples. In the case of copper, the estimated contribution of elastic reverse deformation work

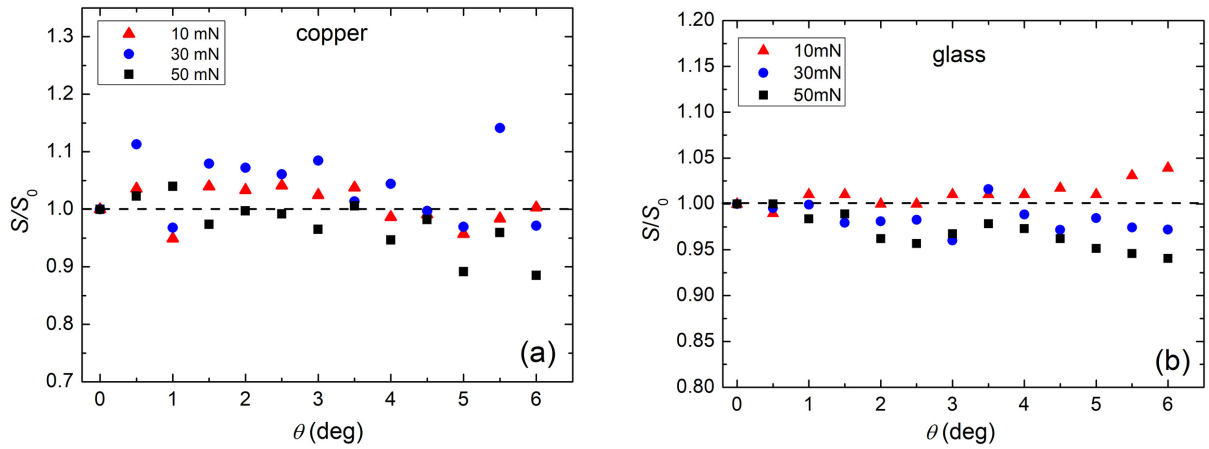

Figure 11. Dependences of experimental normalized stiffness S/S_0 on sample tilt angle θ obtained for 10, 30 and 50 mN of maximum test loads made on (a) copper and (b) glass samples

W_{el} to the total mechanical work of indentation W_{tot} on the horizontal face ($\eta = W_{el}/W_{tot}$) is 7.9%, 8.3% and 9.0% for 10, 30 and 50 mN, respectively. The corresponding values are 51.5%, 52.2% and 53.6% for the above loads in the case of glass. Obviously, in the case of copper, the average contribution of the elastic work to deformation is very low (about 8.4%) and differs by about ±0.5% from the average value for various test loads. However, in the case of glass, this average contribution is much higher (about 52.4%) and differs by about ±1% from the average value for various test loads.

The plots of elastic reverse deformation work W_{el} versus tilt angle θ for copper and glass samples are presented in Figure 12 a and b, respectively, whereas analogous plots made for the contribution of elastic reverse deformation work η are presented in Figure 13 a and b. It should be emphasized that no significant changes were observed for total work W_{tot} in the copper as well as glass case. The plots presented in Figures 12 and 13 show that in the copper case the changes in the W_{el} as well as η are negligibly small. The situation is slightly different in the glass case where the η coefficient slightly increases up to about 3% as tilt angle increases to 6°. Such an increase, for the unchanged value of stiffness S, makes the unloading part of indentation dependency $F(h)$ more curved. It should be added that, the S values depend on the properties used in O-P method. In this experiment the slope S was determined from the tangent fit dF/dh taken for part of unloading curve placed between 40% and 98% of the maximum load. Changing these proportions it is possible to influence on the value S, however, this type of operation does not fall within the scope of this work.

Thus, it may be concluded that the tilt angle leads to insignificant changes in the reduced modulus in copper but this change is much higher in glass. In the latter case, one also observes relatively high increase in the reduced modulus at low applied test loads. For example, at the minimum applied load of

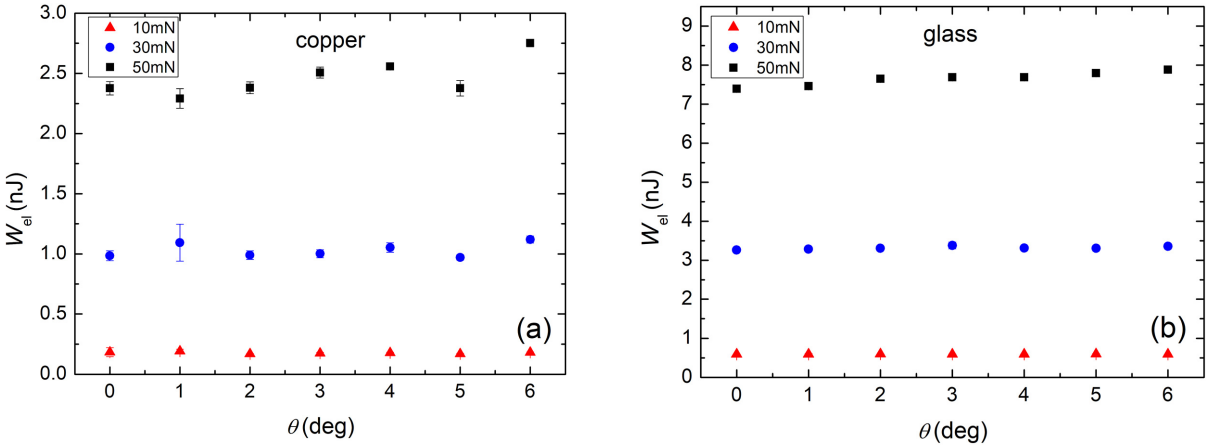

Fig. 12. The plots of elastic reverse deformation work W_{el} versus tilt angle θ for copper and glass samples

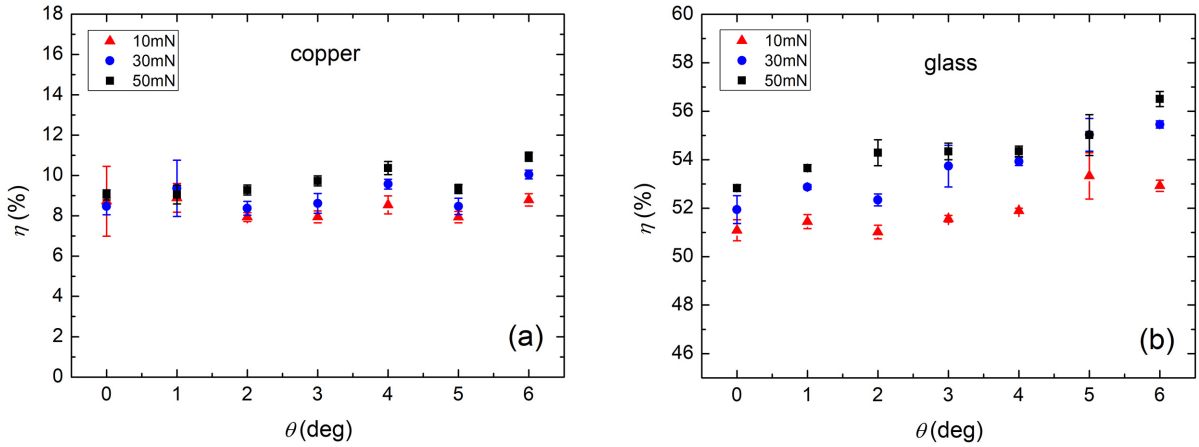

Fig. 13. The plots of contribution of elastic reverse deformation energy to the total energy consumption during indentation η versus tilt angle θ for copper and glass samples

10 mN, the reduced modulus of glass increases by about 5% at $\theta = 5^{o}$. This is consistent with the simulation results obtained for O-P method [8].

CONCLUSIONS

From the indentation experiments carried out in this study on the copper and glass samples at test loads of 10, 30 and 50 mN in the range of tilt angle θ from 0° to 6° the following conclusions may be drawn. Measured indentation hardness H_{IT} increases for tilt angle $\theta > 3^{o}$ and is about 12% at $\theta = 6^{o}$ for copper (pile-up) and glass (sink-in) samples at all applied loads. This increase is comparable with the simulation and experimental results obtained for fused quartz [8,11]. The overestimated values of the hardness of the samples are due to an increase in the projected contact area A with the tilt angle θ when the contact depth h_c is constant, but the theoretical contact area A described by the traditional analytical area function leads to a lower change in the hardness than the experimental one up to about 5%. According to the hypothesis proposed in ref. [8], the disagreement may be associated with the horizontal deflection of the stem holding the indenter. This deflection results in a lower actual penetration depth than that recorded by the instrument. It is shown that Equation (9) relating the stem horizontal deflection d with the tilt angle η of a tilted sample, proposed in this work, satisfactorily explains the above anomalous behaviour. The experimental results of reduced modulus E_r and, consequently, indentation modulus E are less sensitive to the tilt sample than the indentation hardness. In the copper (pile-up) sample the change in E_r is negligible, but in the glass (sink-in and more elastic) sample the increase in E_r is higher at lower loads. At lower loads used in experiment, the results are comparable with the results obtained in ref. [8]. The change in the reduced modulus E_r is mainly due to change in the stiffness S. Small difference between the dependencies E_r and S on the tilt angle θ is due to small influence of change in projected contact area A.

Acknowledgements

The author is grateful to Prof. Keshra Sangwal for his advice and valuable contribution in the preparation of the manuscript. The author is also grateful to the learned referee for his comments and suggestions for improvement in the manuscript.

REFERENCES

1. Mott B.W. Microindentation Hardness Testing, London: Butterworths, 1956.
2. Li H., Ghosh A., Han Y.H., Bradt R.C. The frictional component of the indentation size effect in low load microhardness testing. Journal of Materials Research. 1993; 8(5): 1028–1032.
3. Sangwal K. Review: Indentation size effect, indentation cracks and microhardness measurement of brittle crystalline solids – some basic concepts and trends. Crystal Research and Technology. 2009; 44(10): 1019–1037.
4. Xu Z.-H., Li X. Effect of sample tilt on nanoindentation behaviour of materials. Philosophical Magazine. 2007; 87(16–17): 2299–2312.
5. Gao C., Yao, L., Zheng, R. Liu, M. Effect of sample tilt on spherical indentation of an elastic solid. Journal of Testing and Evaluation 2019; 47(4): 2596–2612.
6. Zhong Y., Li M., Ji B. Effect of sample tilt on indentation and scratch behavior of single crystal copper, Earth and Environmental Science. 2021; 692: 032082.
7. Kashani M.S., Madhavan V. The effect of surface tilt on nanoindentation results. Proc. of ASME, International Mechanical Engineering Congress & Exposition, Seattle, Washington, USA. 2007; 67–71.
8. Kashani M.S., Madhavan V. Analysis and correction of the effect of sample tilt on results of nanoindentation. Acta Materialia. 2011; 59(3): 883–895.
9. Shi C., Zhao H., Huang H., Xu L., Ren L., Bai M., Li J., Hu X. Effects of indenter tilt on nanoindentation results of fused silica: an investigation by finite element analysis, Materials Transactions. 2013; 54(3): 958–963.
10. Wang L., Liu XP. Correlation analysis of surface tilt effect on its mechanical properties by nano-indentation. International Journal of Precision Engineering and Manufacturing. 2019; 22, 327–335.
11. Laurent-Brocq M., Bejanin E., Champion Y. Influence of roughness and tilt on nanoindentation measurements: a quantitative model. Scanning. 2015; 37(5): 350–360.
12. Jakes J.E., Staufer D. Contact area correction for surface tilt in pyramidal Nanoindentation. Journal of Materials Research. 2021; 36(11): 2189–2197.
13. Oliver W.C., Pharr G.M. Measurement of hardness and elastic modulus by instrumented indentation: Advances in understanding and refinements to methodology. Journal of Materials Research. 2004; 19(1): 3–20.
14. Oliver W.C., Pharr G.M. An improved technique for determining hardness and elastic modulus using load and displacement sensing indentation experiments. Journal of Materials Research. 1992; 7(6): 1564–1583.
15. Liu Y., Ngan A.H.W. Depth dependence of hardness in copper single crystals measured by nanoindentation, Scripta Materialia. 2001; 44(2): 237–241.